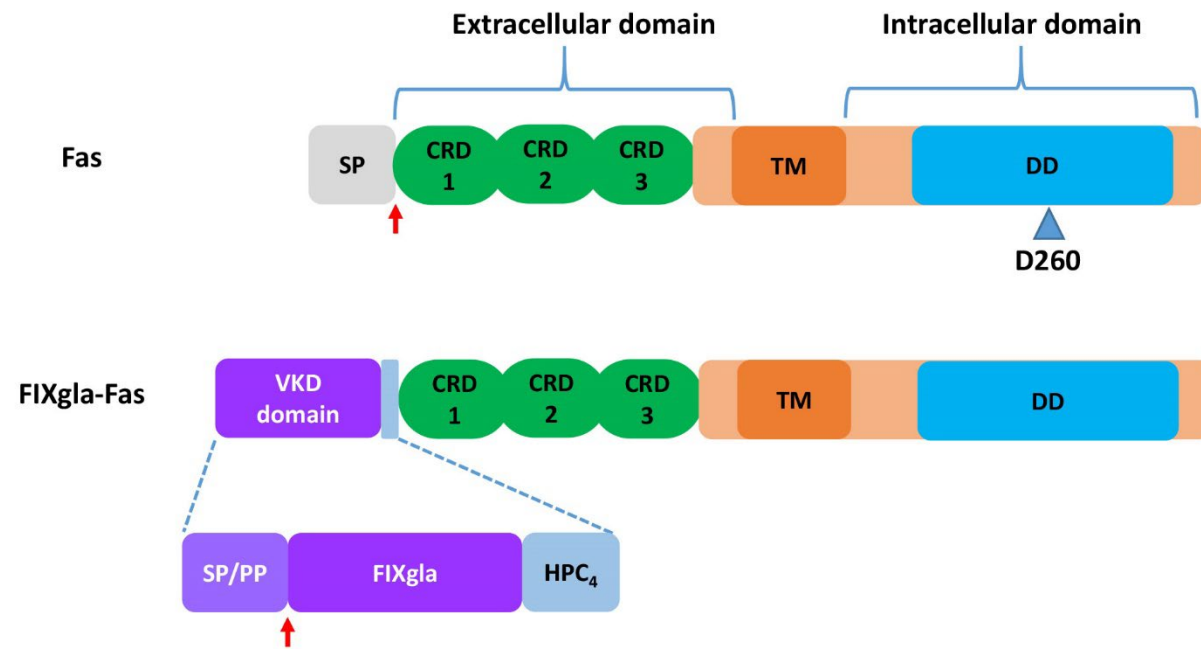
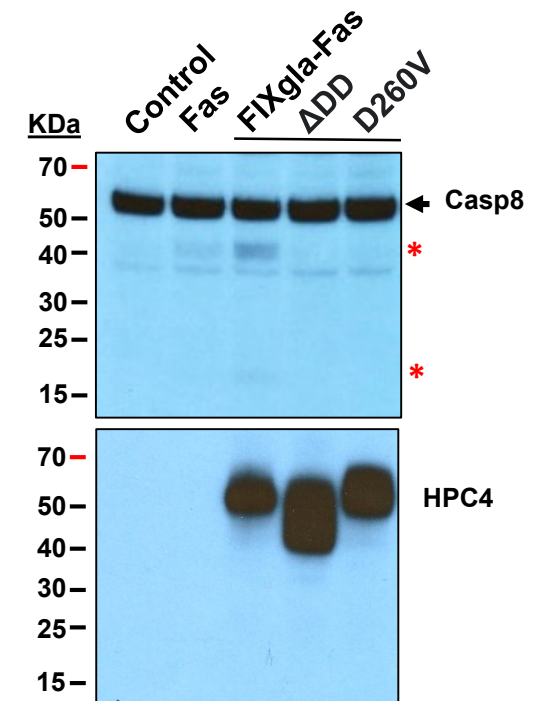
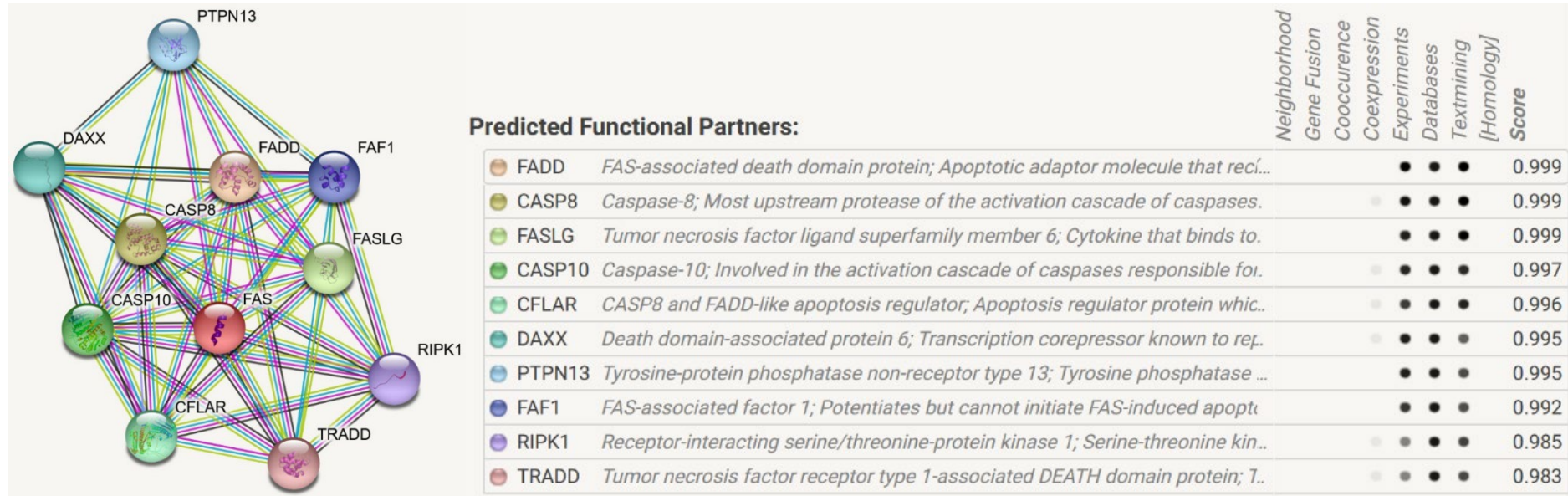
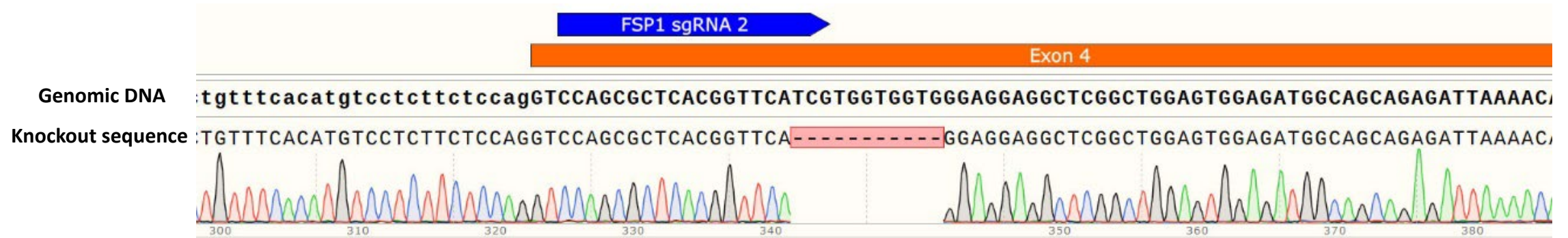


a**b**

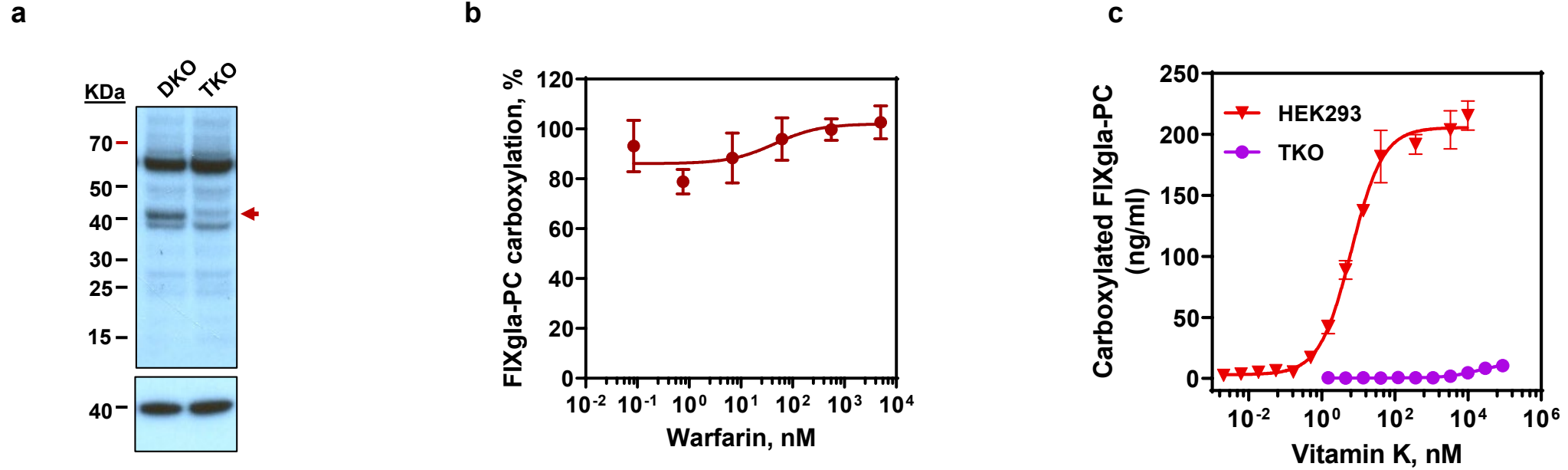
Supplementary Fig. 1 | Vitamin K-dependent apoptotic reporter protein. (a) Schematic diagram of the domain structure of the VKD apoptotic reporter protein FIXgla-Fas. The signal peptide (SP), propeptide (PP), and Gla domain of factor IX (FIXgla) is fused to the extracellular N-terminus of Fas with a HPC4 tag between the two fusion parts for detection purpose. Residue Asp260 within the death domain (DD), important for Fas-FADD interaction, is indicated by a triangle. CRD, cysteine-rich domain; TM, transmembrane domain. Arrowheads indicate positions of the cleavage of signal peptide or propeptide before mature protein is secreted. (b) Effect of FIXgla-Fas reporter protein and its mutants on caspase-dependent apoptosis detected by immunoblotting. The Fas, FIXgla-Fas, the D260V mutant, or FIXgla-Fas with its death domain (DD) deleted (Δ DD) constructs were transiently expressed in HEK293 cells. Transfected cells were incubated with 11 μ M vitamin K for 48 hours before harvesting the cells for immunoblotting. Control: HEK293 cells only. Top: Activation of caspase-8 was probed using anti-caspase-8 antibody. Full-length caspase-8 was indicated by an arrowhead, activated caspase-8 was indicated by asterisks. Bottom: total reporter protein expression probed by anti-HPC4 tag antibody. Similar results were observed at least twice as shown in Fig. 1b.



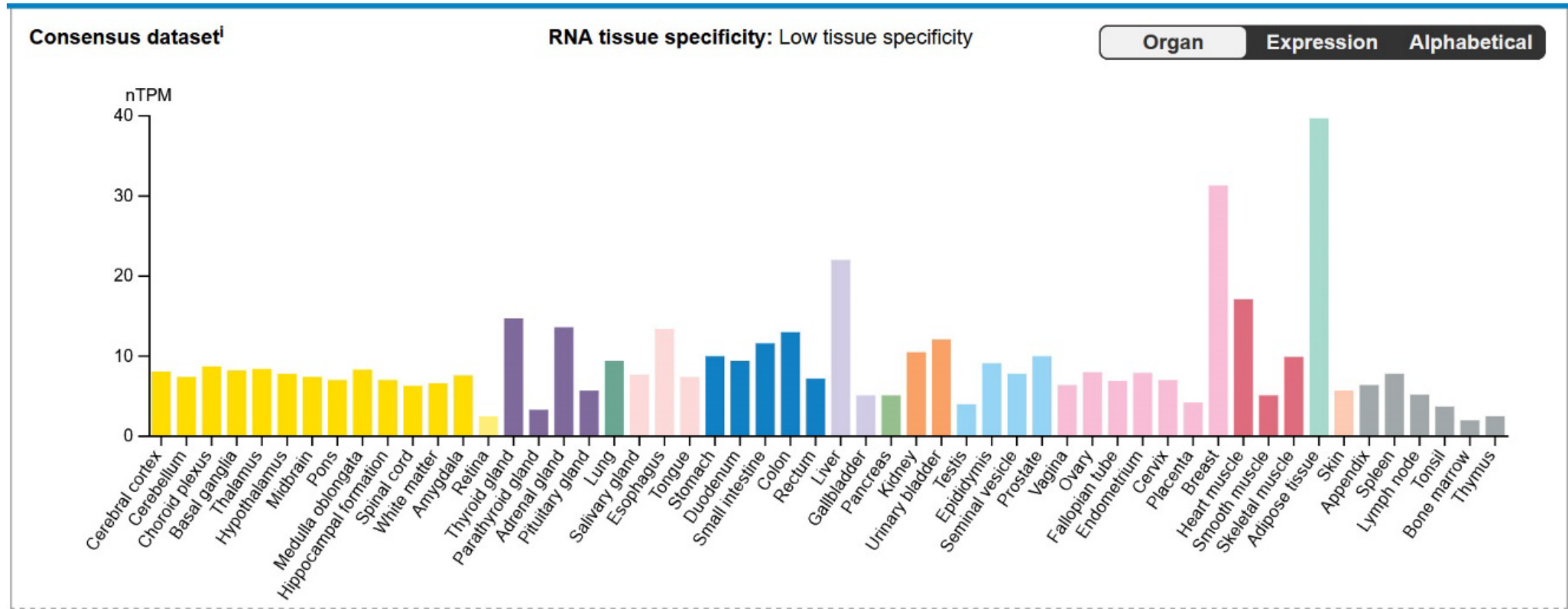
Supplementary Fig. 2 | Network analysis of Fas receptor using the STRING protein-protein interaction network database with default settings. Of the ten proteins that interact with Fas in this network, the sgRNA targeting eight of the proteins (CASP8, CASP10, CFLAR, FADD, FAF1, PTPN13, RIPK1, and TRADD) were enriched in the genome-wide CRISPR-Cas9 loss-of-function VKD screening. Detailed sgRNA enrichment of these genes can be found in Supplementary Table 1.



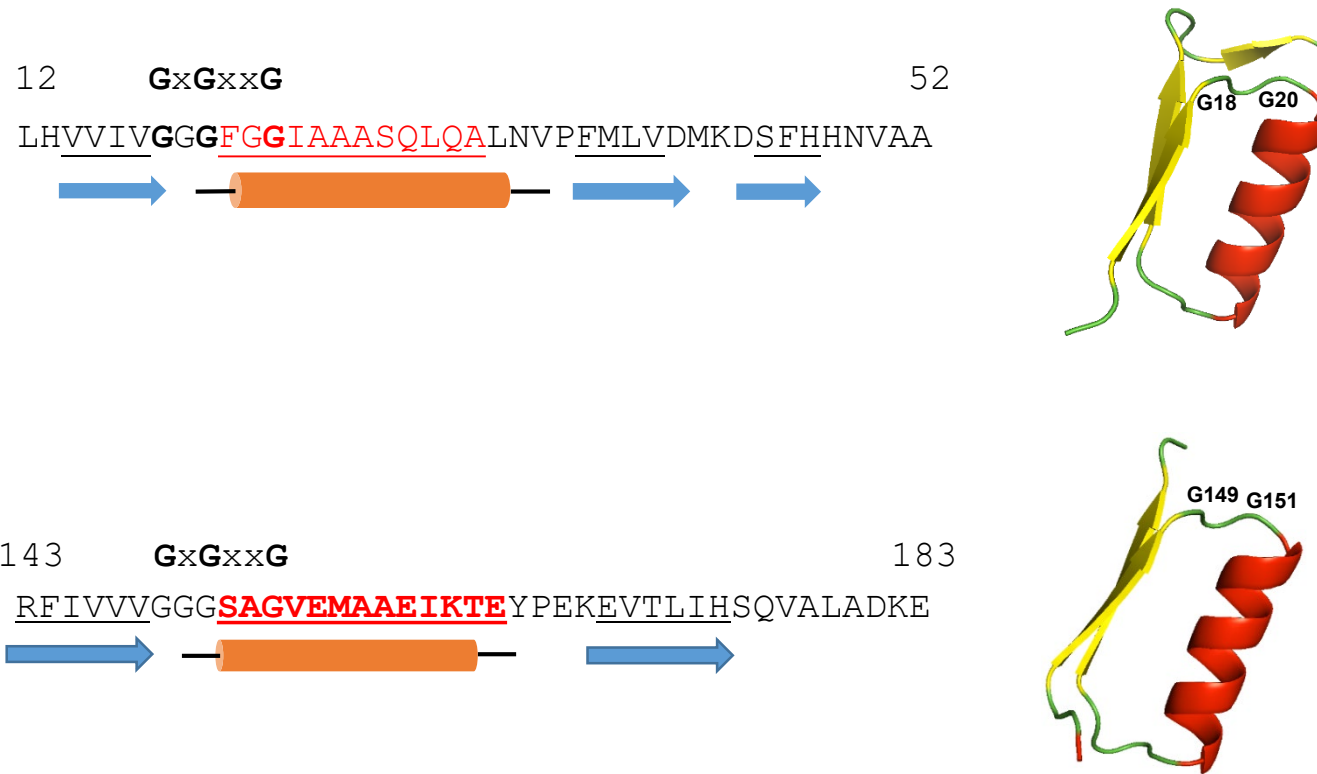
Supplementary Fig. 3 | Genomic DNA sequence analysis of FSP1 knockout HEK293 cells. The sgRNA of CCAGCGCTCACGGTTCATCG (FSP1-2) targeting exon 4 of *fsp1* was used to knock out the endogenous FSP1 in HEK293 cells. After single colonies were obtained, genomic DNA of the FSP1 knockout cells were extracted and used as a template for PCR amplification of the sgRNA targeted region. The sgRNA target sequence is indicated by blue arrows. Intron sequences are in lower case and exon sequences are in upper case. One of the single colonies has one allele has an 11-base deletion (top) while the other has a 1-base insertion (bottom) at the Cas9 cutting site.



Supplementary Fig. 4 | Warfarin and vitamin K concentration titrations in HEK293 and TKO reporter cells. (a) Immunoblotting of DKO cells and these cells with their *fsp1* gene knocked out (TKO). Full-length FSP1 is indicated by an arrowhead. Similar results were observed at least twice. Top: anti-FSP1, bottom: anti-GAPDH. (b) Inhibition of VKD carboxylation in TKO reporter cells. The TKO reporter cells were seeded in a 96-well plate and incubated with increasing concentrations of warfarin in the cell culture medium containing 11 μ M vitamin K for the cell-based activity assay. The carboxylation activity of TKO cells without warfarin in the culture medium was normalized to 100%. Data are presented as mean \pm SD of three independent experiments (n=3). (c) Vitamin K concentration titration of FIXgla-PC/HEK293 (HEK293) and TKO reporter cells. Reporter cells were seeded in 96-well plates and incubated with increasing concentrations of vitamin K for the cell-based activity assay. Carboxylated reporter protein FIXgla-PC in the cell culture medium were determined using ELISA without normalization. Data are presented as mean \pm SD of three independent experiments (n=3).



Supplementary Fig. 5 | Tissue specificity of FSP1 RNA from The Human Protein Atlas Database. A low tissue specificity for the FSP1 gene was determined by The Human Protein Atlas Database (<https://www.proteinatlas.org/ENSG0000042286-AIFM2/tissue>). AIFM2 was the protein name in the database while searching this protein.



Supplementary Fig. 6 | Rossmann fold structural motifs identified in FSP1. Two Rossmann fold motifs were identified in FSP1 between residues 12 to 52 (top) and 143 to 183 (bottom). Rossmann fold motif structure typically contains an alpha helix flanked by two parallel beta strands. The loop connecting the first beta strand with the alpha helix contains the consensus sequence GxGxxG, which established direct interaction with the dinucleotide cofactor. Rossmann fold structures were obtained by Pymol using AlphaFold predicted model. Conserved glycine residues within the GxGxxG sequence that have been mutated in this study were indicated in the structure model.

MG---S-----VV-VGGGFGG--AA--L-----L-D--D-FHHNV-ALRA-V--GFA--TFI-----F--F-Q-

Table with 30 rows and 80 columns of amino acid sequences. Row 1: MGSQVSVESGALHVVIVGGGFGGIAAASQLQALNVPFMLVDMKDSFHNNVAALRASVETGFAKKTFFISYSVTFKDNFRQG. Row 30: MGGSLSIDD-GVHVIVGGGFGGIAAAQLKYRVPFTIIDLRDAFHNNVASLRASVQSGFAKQTFIPFRETFGDSFLQG.

-V---D-----V-L-----SHLIL-TG--G-FPGK-----AI--YE-----VGGG--GVEMAAE

Table with 30 rows and 160 columns of amino acid sequences. Row 1: LVVGLDLKNQTVLLQGGREALPFSHLILATGSGTGFPGKFNQVSSQQAIIQAYEDMVRQVQRSFIVVVGGGSAGVEMAAE. Row 30: RVARVDTSAQIVVLEDGKEVHYSHLILCTGTDGPFPGKYNLASYQTAIEKYEFEVKEVQAAGTVLVVGGGSTGVEMAAE.

--T---K-V-L-H-----AD--LL--V---K--L---V-L-L--V-N-----N-----T-K-----V

	170	180	190	200	210	220	230	240
1	IKTEYPEKEVTLIHSQVALADKELLPSVRQEVREILLRKGVQLLLSERVSNLEELPLNEYREYIKVQTDKGTEVAT-NLV	239						
2	LKTDYPEKEVTLIHSKVPLADPELLPCVRQEVKEILLQKGVVELLLSERVSNLEELPLNECRDSIQVKTDKGTQLAA-NLV	238						
3	IKTEYPEKEVTLIHSQVALADKELLPCVRQEVKEILLRKGVQLLLSERVSNLEELPVNEYREYIKVQTDKGTEVAT-NLV	239						
4	VKTMYPTEKEVALIHSKIALADEELLPRVRQEVKETLIHEGVNLF LGQRVDNLHELTLHQFKENMVVKTDKGTEMTV-DLV	238						
5	IKTEFHDKKVVLIHPREEVADPELLPCVKEQAKQVLLLEKGVVELLLGQKVSNLEELPLNVCRSGMVVKTNKNEQVTT-DLV	238						
6	VKTEFPEKEVTLIHSQVALADKELLPCVRQEAKEILLQKGVQLLLSERVSNLEELPLNEYRERIQVHTDKGTEVAT-NLV	239						
7	VKTTYPNKEVTLVHSKMALADGGLPRVREAVKETLTQQGVHLLLGQKVSNLHMLSLNQFKENMMVKTDKGTEVAA-DLV	238						
8	VKTKYPNKEVTLIHSKVALADAELPRVRQEVKESLLKEGVHLLLSQKVENLQSLTLNQFKENMIVKTDKGTEIVT-DLV	238						
9	IKSDYPQKEVTLIHSKVALADVELPSVRQTVKEILLRKGVKLLLSQRASNLTLQLKLVNEVQEQMSVETDKGTTVTA-DLV	238						
10	IKTDYDPEKEVTLIHSKIALADIELPSVRQGVKEILLKGGVQLLELQGVKVTNLKELVTNETKNDQKVLTDKGLEFNA-DLV	238						
11	VKTDYPEKEVTLVHSKVALADVQLQPKVRRTVKEILLSKGVRLLLAQKVTNLDQVTSNVAQENTVLQLDKNSEVVTCDLV	239						
12	IKTEYPEKEVTLIHSRVPLADKELLPCVRQEVKEILLRKGVQLLLSERVSNLEELPRNEYREYIKVETDKGTEVAT-NLV	239						
13	IRTEFTDKKVVLIHPREEVADPDLLPSVKEQAKQVLLLEKGVVELLLGRKVTNLDELELVNCRKGMVKTNKNEQVTA-DLV	238						
14	IKTEYPGKEIILIHSTALADVELPSVRQVVKEILLRKGVRLLSEKVS DIENLRPNQFQKDMVVRTDKGTEVVV-DLV	238						
15	IKTEYPAKEVTLIHSKIALADVELQSVRQEVKEILLRKGVRLLSEKVS NVENLTTNQFQKDMVVRTDKGTEVVV-DLV	238						
16	IKTEYPAKEVTLIHSKIALADVELPSVRQEVKEILLRQVHLLSERVQNMHTLTLNQFQENMAVKTDKGREVAA-DLV	238						
17	IRTEYDQKVVVHVRMQLADPDLLPIVRYQAKEVLLLEKGVVELLLGHKVSNLSELKLNATTKNMEVTTDKGERIKT-DLV	237						
18	IKTEFPEKEVTLIHSQVALADKELLPCVRQEAKEILLQKGVQLLLSERVMNLEQLPLNEYRERIQVHTDKGTEVAT-NLV	239						
19	IKTEYPAKEVTLIHSKVALADVELPSVRQEVKEILLRKGVRLLSERVSNLEKFTPNCFQKDMVVRTDKGTEIVT-DLV	238						
20	VKTEFPEKEVTLIHSQVALADKELLPCVRQEAKEILLQKGVQLLLSERVSNLEELPLNEYRECIQVHTDKGTEVAT-NLV	239						
21	IKTEYPEKEVTLIHSKMALADTELLPCVRQEVKEILLRKGVQLLLSERVSNLEALPVNEHRECIKVQTDKGTEVDA-NLV	239						
22	IKTEYPEKEVTLIHSQVALADKELLPCVRQEAKEILLRKGVQLLLSERVSNLEELPLNEYQECIKVQTDKGTEVAA-NLV	239						
23	IKTEYPEKEVTLIHSKVPLADQELLPCVRQEVKEILLRKGVQLLLSERVSNLEELPLNEYREYIKVQTDKGTEVAT-NLV	239						
24	IKTEYPAKEVTLIHSKIALADVELPSVRQMVKEILLKKEVRLLSDRVSNLHMLTLNRFQENMAVKTDKGTEVAA-DLV	238						
25	ISTKXPSKEVTIHSKIPALADAELLPRVRQEVKETLIQEGVHLLLNHKVSNLDKLTNLNQFKENIVVETDKGTEVVT-DLV	238						
26	IKTEYDQKEVTLIHSQVPLADKELLPCVRQEVKEILLRKGVQLLLSERVSNLEELPLNEYREYIKVQTDKGTEVAT-NLV	239						
27	IKTEYPEKEVTLIHSQVALADKELLPCVRQEAKEILLRKGVQLLLSERVSNLEELPLNEYRECIKVQTDKGTEVAA-NLV	239						
28	IKTEYPAKEVTLIHSKIALAEVELLSVRQEVKEILLRKGVRLLSERVSNLENFTPNQFQKDMVVRTDKGTEVIA-DLV	238						
29	IKTEHPEKEVTLIHSQVALADKELLPCVRQEAKEILLRKGVQLLLSERVSNLEELPVNEYRECIKVQTDKGTEVAT-NLV	239						
30	IKTEFPDKKVVLIHSRVPLADPELLPSVREQAKEVLLQKGVVELLLEQKVTNLDLELVNTRKDIVIKTDKDEITA-DLV	238						

--C-G---NS-AY---F---LASNGAL-VNE-LQVEGY-NIYAIGDCADVKEPKMAYHAGLHANVAVTNI-NSL-QKPLK

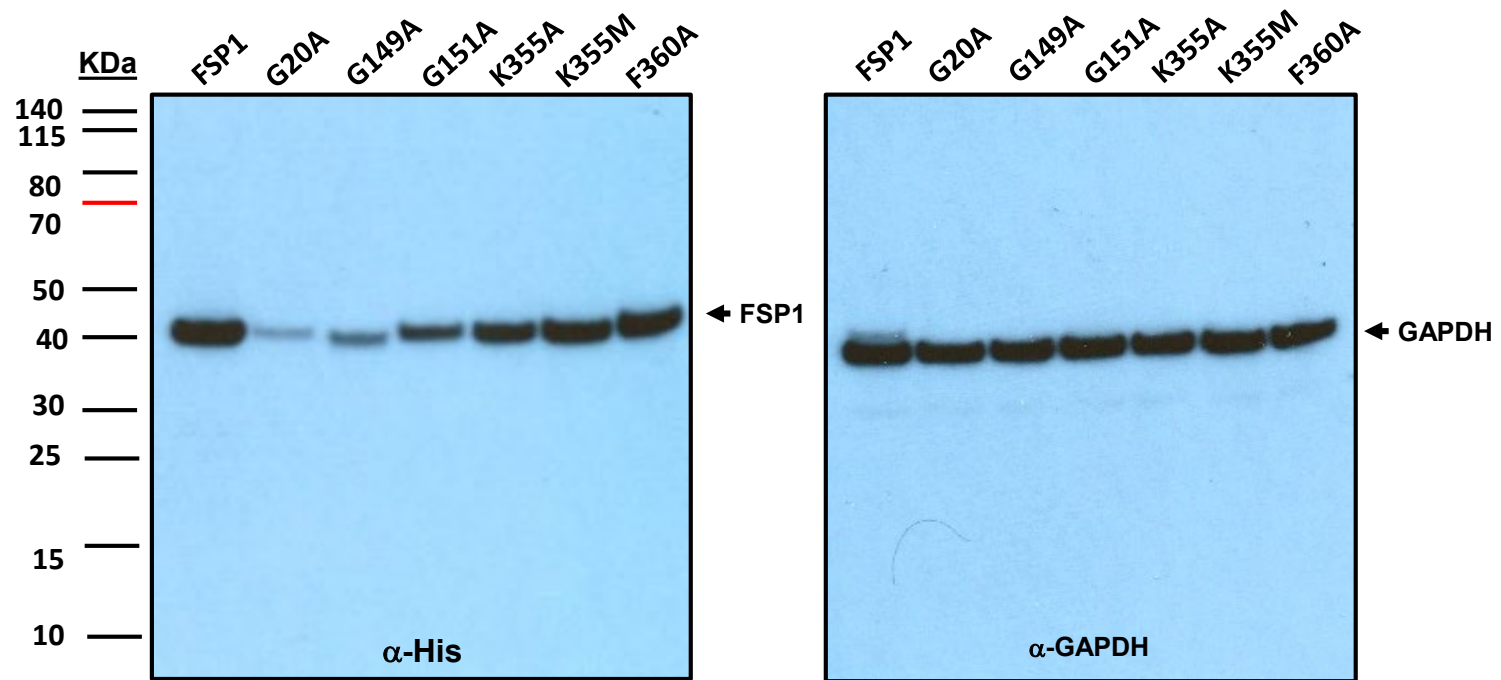
	250	260	270	280	290	300	310	320
1	ILCTGIKINSSAYRKAFESRLASSGALRVNEHLQVEGHSNIYAIGDCADVTPKMAVLAGLHANIAVANIVNSVKQRPLQ	319						
2	ILCNGIKINSSAYSSALGDQADNGALMVNDHLQVQGFNSIYAIGDCANVKEPKMAYHAGLHANVVVTNIIVNSLKQKPLK	318						
3	IPCNGIKVNSSAYCSAFESRLASNGALQVNEYLQVEGYSNVYAIGDCADVKEPKMAYHAGLHANIVTTNIINSMKQRPLK	319						
4	ILCTGIKINSSAYRSSFINKLASNGALKVNNDHLQVEGYDNIYAIGDCADVKEPKMAYHAGLHADVAVTNIINSLTQKPLK	318						
5	ICCTGSKINSEAYRSSMSSCLAENGALKVNKHLQVEGFNVYAVGDCANLSEPKMAYHAGLHAGVAATNIINSLSGKALT	318						
6	IVCNGIKVNSSAYHSAFDGHLASNGALRVNEYLQVEGYSHIYAIGDCADVKEPKMAYHAGLHASVAVANIVNSRKQRPLK	319						
7	ILCTGIKINSSAYSSAFRDQLANNGALKVNNDYLVQVGYDNIYAIGDCSDVKEPKMAYHAQLHANVVVTNIINSLTEKPLK	318						
8	ILCTGIKINSSAYSSAFSDKLASNGALQVNEYLQVKGVDNIYAIGDCADVNEPKMAYHAGLHADVAVTNIIVNSLTQKPLK	318						
9	ICCTGIKINSSAYSNAKLKLDNGALRVNEHLQVEGHSNIYAIGDCADVKEPKMAYHAGLHAKVAVKNIIVNSLTQKPLA	318						
10	ICCTGIKINSSAYENSFKDAIVKNGALMVNDYLVQVEGSHIYAIGDCADVKEPKMAYHAGLHAGVAVDNIINTLKEKPLK	318						
11	LCCTGYKISSSSYSAFQDKLAEDGALIVNDYLVQVGHANVYAVGDCAYINEPKMAYYAGIHARVAATNVRNSLIGKSLK	319						
12	IVCNGIKINSSAYRSAFESRLASNGALKVNNEFLQVEGYSNIYAIGDCADTKEPKMAYHAGLHANVAVANIVNSMKQRPLK	319						
13	ICCTGNKINSEAYRSSLTTCMAESGALKVNQHLQVEGFNVYAVGDCANLDEPKLAYHAGLHAAVAATNIINSLTGKCLT	318						
14	VLCTGIKINSSAYAAAFQDKMASDNGALKVNKHLQLEGYENIYAIGDCADLKEPKMAYHAGLHANVVVTNIINSLTQKPLK	318						
15	VLCTGIKINSSAYATAFQDKLASNGALNVNKHLLQLEGYDNIYAIGDCANLKEPKMAYHAGLHANIVVSNINSLTHKPLK	318						
16	ILCTGIKINSSAYSSAFGEKLASNGALKVNQYLQVEGYDNIYAIGDCADVKEPKMAYHAGLHANIVVTNIINSLTQKPLK	318						
17	FCCTGLRVNSSAYKSSFSDHMTNSGALKVNNEHLQVEGFSNVFAIGDCNNVNEAKTAYNAELHAGIAGVNIANSVNGKRLT	317						
18	IVCNGIRINSSAYRSASFESHLAGNGALRVNEYLQVEGCSHVYAIGDCADVKEPKMAYHAGLHASVAVANIVNSARKQRPLK	319						
19	ILCTGIKINSSAYGSFQDKMASNGALRVNQHLLQLEGYENIYAIGDCADLKEPKMAYHAGLHANVVVTNIIVNSLKNKSLQ	318						
20	IVCNGIKINSSAYHSAFDSHLASNGALRVNEHLQVEGCSRVAIYIGDCADVKEPKMAYHAGLHAGIIVANIVNSMKQRPLK	319						
21	IVCNGIKINSSAYRSAFQDRLASNGALRVNEYLQVEGYSHIYAIGDCADVREPMAVHASLHANVAVANIVNSMKQRPLK	319						
22	IVCNGIKINSSAYRSAFDDGLASNGALKVNNEYLQVEGCSHVYAIGDCADVKEPKMAYHAGLHANVAVANIINSMKQRPLK	319						
23	IVCNGIKINSSAYCSAFESRLASNSALRVNEYLQVEGYSNIYAIGDCADVKEPKMAYHAGLHANIVTTNIIVNSMKQRPLK	319						
24	ILCTGIKINSSAYSSAFQDKLASNGALKVNQYLQVEGYDNIYAIGDCADVKEPKMAYHAGLHANIVVTNIINSLTQKPLK	318						
25	ILCTGIKINSSAYRSAFSDKLAKNALQVNEHLQVKGYSNIYAIGDCAXVREPMAVHASLHADVAVANIVNSLTKNPLK	318						
26	ILCNGIKINSSAYSSAFESRLASNGALRVNEFLQVEGYSNIYAIGDCADVKEPKMAYHAGLHANVAVTNLVNSMKQRPLK	319						
27	IVCNGIKINSSAYRSAFDDGLASNGALKVNNEYLQVEGCSHVYAIGDCADVKEPKMAYHAGLHANVAVTNIINSMKQRPLK	319						
28	ILCTGIKINSSAYASAFADKLASNGALKVNQHLLQLEGYENIYAIGDCADLKEPKMAYHAGLHANIVVTNIINSLTHKSLK	318						
29	IVCNGIKINSSAYRRFAFASQLASNGALPVNEYLQVEGCSHVYAIGDCADVKEPKMAYHAGLHANVAVANIINSTQRPLK	319						
30	ICCTGNKINSSAYSSSLSECLAEEDGSLNVNEHLQVTFQNVYAVGDCANIKEPKMAYHAGLHGGVAATNIINNSLGGKPLT	318						

-Y-PG-LTFLLSMGRNDGVGQISG-YVGR-LV--AKSRDLFVSKSWKTM-Q--P--

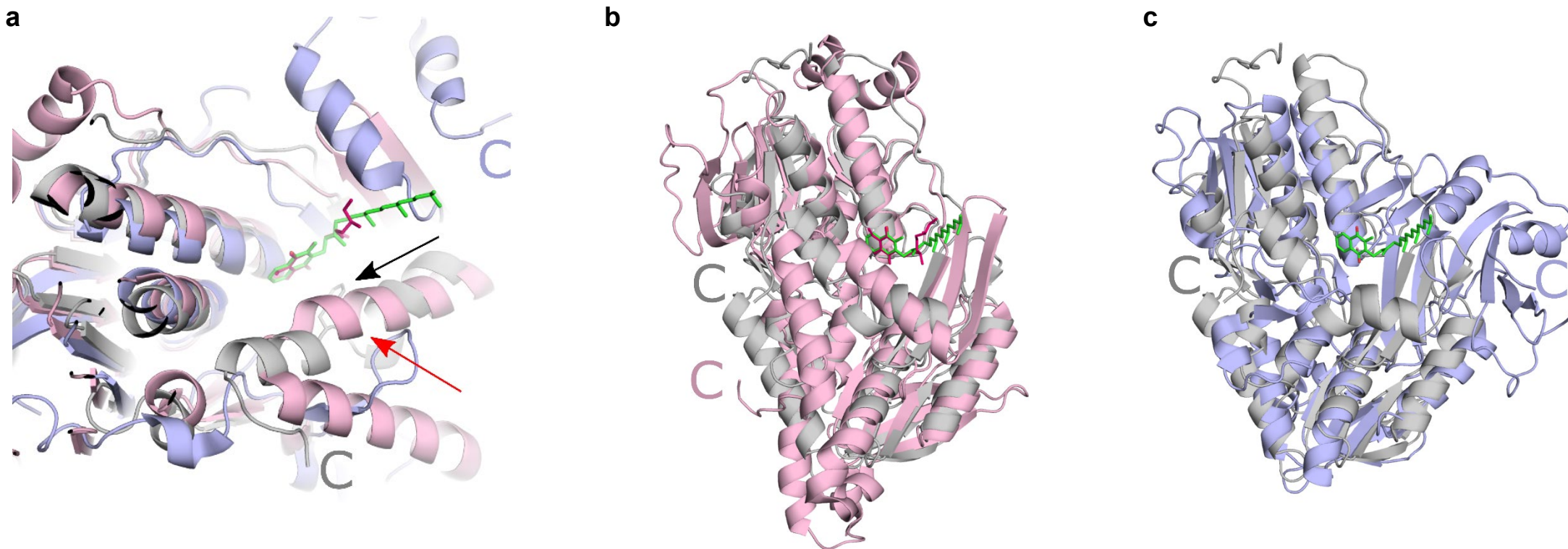
	330	340	350	360	370		
1	AYKPGAL	TFLLSMGRNDGVGQISGF	YVGR	LMVRLTKSRDLFVST	SWKTM	RQSPP-- 373	
2	TYKPGAL	TFLLSMGRNDGVGQISGF	YVGR	LVRFAKSRDLFVST	SWKTM	RQTAPS- 373	
3	AYKPGAL	TFLLSMGRNDGVGQISGF	YVGR	LMVQLLTKSRDLFVST	SWKTM	RQSPP-- 373	
4	IYTPGSL	TFLISMGSNDGVGQISGI	YVGR	LIVTAKSKDLFVSKSWK	KMG	QHMP- 373	
5	SYKTGNV	TMLIAMGKDA	GVGQFNGYKLP	RFVLT	KGKSEGLLLW	KSWREMGQKAPN- 373	
6	AYKPGAL	TFLLSMGRNDGVGQISGF	YVGR	LMVRLAKSRDLFVSS	SWKTM	RQSPP-- 373	
7	IYKPGSL	TFLISLGSNDGVGQISEY	YVGR	LIVTLKSKDLFIS	SKSWK	KMHQHMP- 373	
8	TYTPGSL	TFLISLGRCDGVGQISDY	YVGR	LIVTVVKSRLDFV	QSWRK	MGCMP- 373	
9	AYEPGR	LTMLLSMGRNDGVGQISNC	YVGR	LIVVMAKSRGLLV	WKS	WAMGQCVPS- 373	
10	VYNPGAL	TMLLSLGRD	GGIGQLYGFHAGK	FIVTLAKSKDLMV	WKS	WEMDQAI- 373	
11	TYKPGAL	SMLLSMGRNDGVGQFNG	CYLGRFF	VTTAKSRDIFVSK	SWK	EMGQTM- 374	
12	AYKPGAL	TFLLSMGRNDGVGQISGF	YVGR	LMVRLAKSRDLL	IST	SWKTM	RQSPP-- 373
13	SYRTGNV	TMLIAMGKDA	GVGQFNGYKLP	RFVLT	KGKSQSLLLW	KSWREMGQKAPN- 373	
14	TYEPGSL	TFLLSMGRNDGVGQVNG	YVGR	LIVTIAKSRDLFVSK	SWR	TMGQTMPS- 373	
15	TYQPGSL	TFLLSMGRNDGVGQVKG	YVGR	LIVTIAKSRDLFVSK	SWK	TMGQMP- 373	
16	TYQPGSL	TFLLSMGRNDGVGQISG	CYVGR	LIVTIAKSRDLFVSK	SWK	TMGQTM- 373	
17	AYRTGNV	TMLLAMGRD	GGVGVNGFQLP	RCLVALLKSRDLLLW	KSWRE	MKQKQPT- 373	
18	AYKPGAL	TFLLSMGRNDGVGQISGF	YVGR	LMVRLAKSRDLFVSS	SWKTM	RQSPP-- 373	
19	AYQPGSL	TFLLSMGRNDGVGQING	YVGR	LIVTTAKSRDLFVYK	SWK	TMGQMP- 373	
20	AYKPGAL	TFLLSMGRNDGVGQISGF	YVGR	FMVRLAKSRDLFVSS	SWK	TMRQSPP-- 373	
21	TYKPGSL	TFLLSMGRNDGVGQISG	FYVGR	LMVRLAKSRDLLVST	SWK	TMKQSP- 373	
22	AYRPGAL	TFLLSMGRNDGVGQISG	FYVGR	LMVRLAKSRDLFIS	SSW	KTM	RQSPP-- 373
23	AYKPGAL	TFLLSMGRNDGVGQISG	FYVGR	LMVRLAKSRDLFVST	SWK	TMR	RQSPP-- 373
24	TYQPGSL	TFLLSMGRNDGVGQING	CYVGR	LIVTIAKSRDLFVSK	SWK	TMGQTM- 373	
25	TYTPGSL	TFLISLGRNDGVGQING	YVGR	LIVTAVKSKDLFVSK	SWR	KMHQCM- 373	
26	AYKPGAL	TFLLSMGRNDGVGQISG	FYVGR	LMVRLAKSRDLFVST	SWK	TMR	RQSPP-- 373
27	AYRPGAL	TFLLSMGRNDGVGQISG	FYVGR	LMVRLAKSRDLFIS	SSW	KTM	RQSPP-- 373
28	TYQPGSL	TFLLSMGRNDGVGQING	CYVGR	LIVTIAKSRDLFVSK	SWK	TMGQTM- 373	
29	AYKPGAL	TFLLSMGRNDGVGQISG	FYVGR	QFMVRLAKSRDLFVST	SWK	TMR	RQSPP-- 373
30	SYRPGNV	TMLLAMGRD	GGVGVNGYKLP	RFVLT	QGKSKG	LLW	KSWRDMGQSAPS- 373

- tr H2Q210 H2Q210_PANTR Apoptosis inducing factor mitochondria associated 2 O=S=Pan troglodytes OX=9598 GN=AIFM2 PE=2 SV=1
- tr A0A4X2LCH5 A0A4X2LCH5_VOMUR Apoptosis inducing factor mitochondria associated 2 O=S=Vombatus ursinus OX=29139 GN=AIFM2 PE=4 SV=1
- tr G3TFJ2 G3TFJ2_LOXAF Apoptosis inducing factor mitochondria associated 2 O=S=Loxodonta africana OX=9785 GN=AIFM2 PE=4 SV=1
- tr G1KUD7 G1KUD7_A NOC A L-amino-acid oxidase O=S=A nolis carolinensis OX=28377 GN=aifm2 PE=3 SV=2
- tr E7FFC4 E7FFC4_DANRE Apoptosis-inducing factor mitochondria-associated 2 OS=Danio rerio OX=7955 GN=aifm2 PE=1 SV=1
- tr E2RQW8 E2RQW8_CANLF Apoptosis inducing factor mitochondria associated 2 O=S=Canis lupus familiaris OX=9615 GN=AIFM2 PE=4 SV=1
- tr A0A6J1UCF5 A0A6J1UCF5_9SAUR L-amino-acid oxidase OS=Notechis scutatus OX=8663 GN=A IFM2 PE=3 SV=1
- tr A0A670I7A9 A0A670I7A9_PODMU L-amino-acid oxidase OS=Podarcis muralis OX=64176 GN=A IFM2 PE=3 SV=1
- tr M3XJX5 M3XJX5_LATCH P yr_redox_2 domain-containing protein O=S=Latimeria chalumnae OX=7897 GN=A IFM2 P E=4 SV=1
- tr A0A4W3HBPO A0A4W3HBPO_CALMI Pyr_redox_2 domain-containing protein OS=Callorhinchus milii OX=7868 GN=aifm2 PE=4 SV=1
- sp B4F6I3 FSP1_XENTR Ferroptosis suppressor protein 1 OS=Xenopus tropicalis OX=8364 GN=aifm2 P E=2 SV=1
- sp Q8BUE4 FSP1_MOUSE Ferroptosis suppressor protein 1 OS=Mus musculus OX=10090 GN=Aifm2 PE=1 SV=1
- tr A0A672QUN3 A0A672QUN3_SINGR Apoptosis inducing factor mitochondria associated 2 O=S=Sinocyc locheilus grahmi OX=75366 GN=aifm2P E=4 SV=1
- sp B5FXE5 FSP1_TA EGU Ferroptosis suppressor protein 1 O=S=Taeniopygia guttata OX=59729 GN=A IFM2 P E=2 SV=1
- tr E1BR24 E1BR24_CHICK P yr_redox_2 domain-containing protein O=S=Gallus gallus OX=9031 GN=A IFM2 P E=4 SV=1
- tr K7G371 K7G371_PELSI Pyr_redox_2 domain-containing protein OS=Pelodiscus sinensis OX=13735 GN=AIFM2 PE=4 SV=1
- tr A0A3B5KF37 A0A3B5KF37_TAKRU Pyr_redox_2 domain-containing protein O=S=Takifugu rubripes OX=31033 GN=aifm2 PE=4 SV=1
- tr A0A6G1AF34 A0A6G1AF34_CROCR A IFM2 factor (Fragment) O=S=Crocota crocata OX=9678 GN=A ifm2 PE=4 SV=1
- tr A0A7K4LBN8 A0A7K4LBN8_9AVES A IFM2 factor (Fragment) O=S=Cryptorellus undulatus OX=48396 GN=Aifm2 PE=4 SV=1
- tr A0A2U3ZUK2 A0A2U3ZUK2_ODORO apoptosis-inducing factor 2 OS=Odobenus rosmarus divergens OX=9708 GN=AIFM2 PE=4 SV=1
- tr A0A6P5AS70 A0A6P5AS70_BOSIN apoptosis-inducing factor 2 O=S=Bos indicus OX=9915 GN=AIFM2 PE=4 SV=1
- tr A0A6I9IIM4 A0A6I9IIM4_VICPA apoptosis-inducing factor 2 isoform X1 OS=Vicugna pacos OX=30538 GN=AIFM2 PE=4 SV=1
- tr A0A6I9J4K1 A0A6I9J4K1_CHRAS apoptosis-inducing factor 2 O=S=Chrysochloris asiatica OX=185453 GN=AIFM2 PE=4 SV=1
- tr A0A8C3ISU4 A0A8C3ISU4_CHRPI Apoptosis inducing factor mitochondria associated 2 O=S=Chrysemys picta bellii OX=8478 GN=AIFM2 PE=4 SV=1
- tr A0A8D0DNU7 A0A8D0DNU7_9SAUR Apoptosis inducing factor mitochondria associated 2 O=S=Salvator merianae OX=96440 GN=AIFM2 PE=4 SV=1
- tr A0A8C5Z5X0 A0A8C5Z5X0_MARMA Apoptosis inducing factor mitochondria associated 2 O=S=Marmota marmota marmota OX=9994 GN=AIFM2 P E=4 SV=1
- tr A0A8B7K828 A0A8B7K828_CAMFR apoptosis-inducing factor 2 isoform X1 OS=Camelus ferus OX=419612 GN=A IFM2 PE=4 SV=1
- tr A0A8B7JL1 A0A8B7JL1_9AVES apoptosis-inducing factor 2 isoform X1 OS=Apteryx mantelli mantelli OX=202946 GN=AIFM2 PE=4 SV=1
- tr A0A671EWY5 A0A671EWY5_RHIFE Apoptosis inducing factor mitochondria associated 2 O=S=Rhinolophus ferrumequinum OX=59479 GN=AIFM2 P E=4 SV=1
- tr A0A6J2V437 A0A6J2V437_CHACN apoptosis-inducing factor 2 isoform X2 OS=Chanos chanos OX=29144 GN=aifm2 PE=4 SV=1

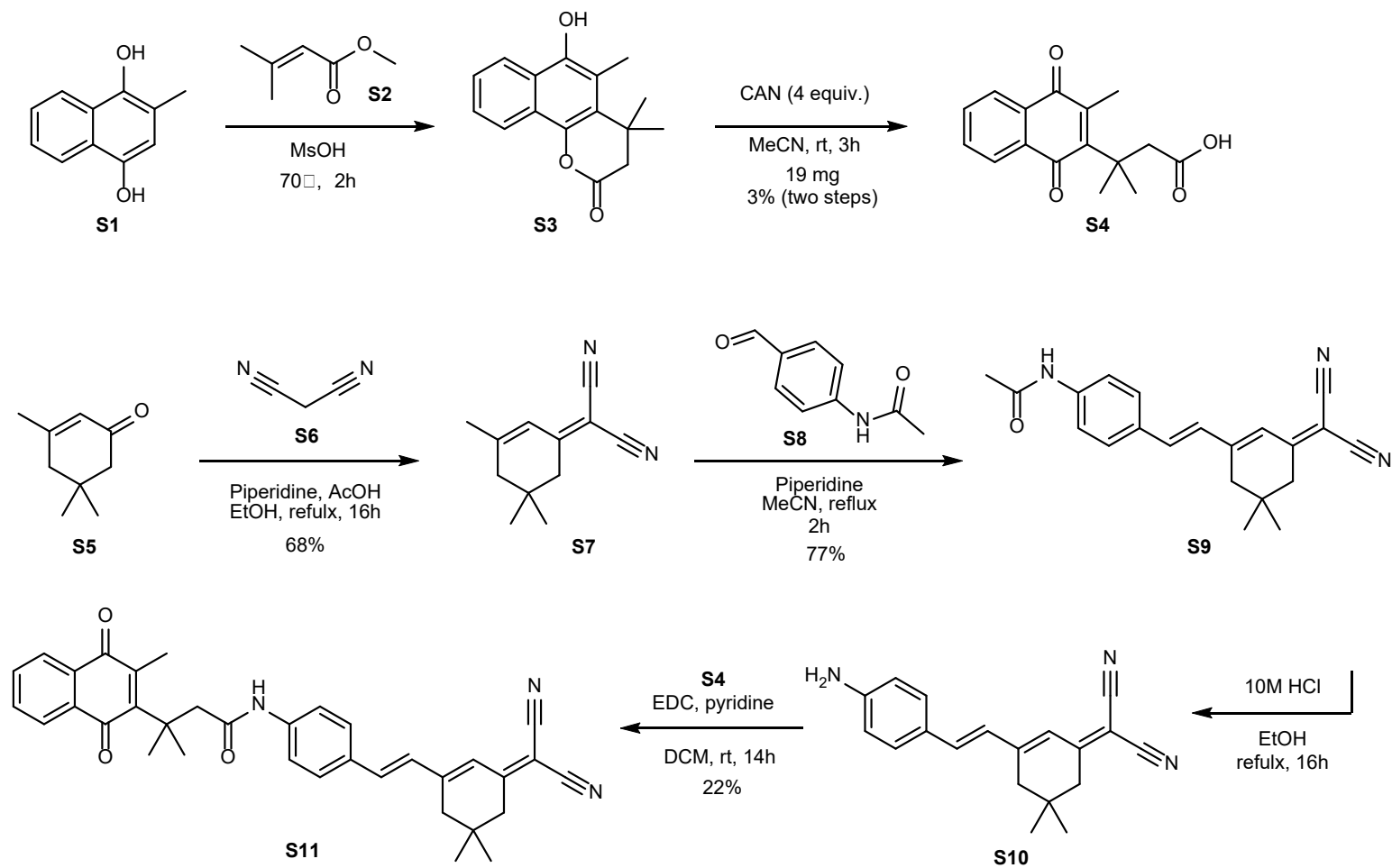
Supplementary Fig. 7 | FSP1 sequence alignment from 30 diverse species using SnapGene. Conserved sequences are highlighted in yellow. Consensus threshold was set as 95%. Residues mutated for functional study in this paper are indicated by asterisks. The GxGxxG conserved consensus sequences within the Rossmann fold are underlined.



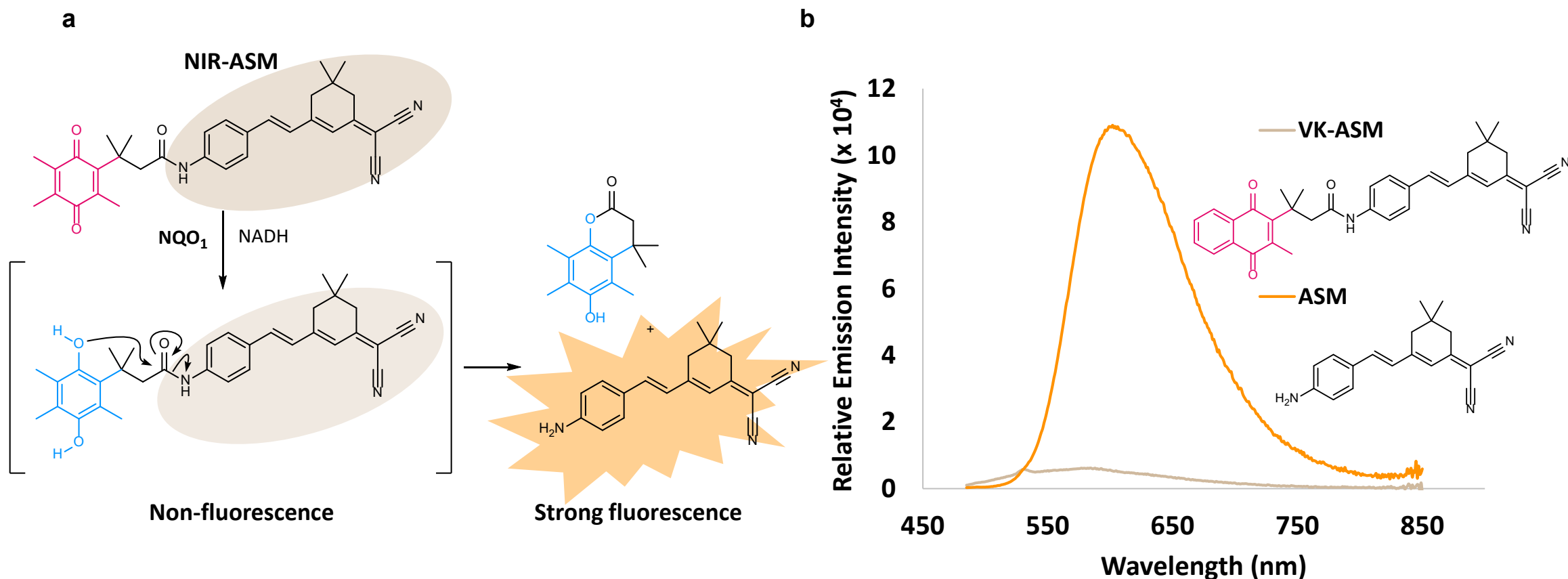
Supplementary Fig. 8 | Immunoblotting of FSP1 and its mutants with a His-tag at the C-terminus. His-Tagged FSP1 and its mutants were transiently expressed in HEK293 cells. Forty-eight hours post-transfection, transfected cells were harvested and the cell lysates were used for SDS-PAGE electrophoresis. Protein bands were transferred to PVDF membrane and probed by anti-His antibody (left) or anti-GADPH antibody as described in the Methods. Similar results were observed at least twice times as shown in these blots.



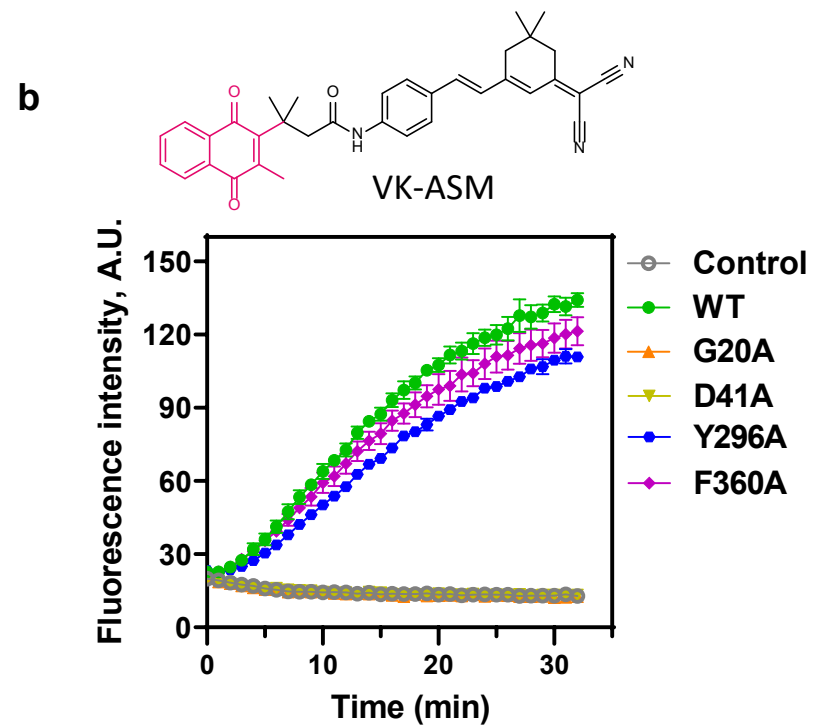
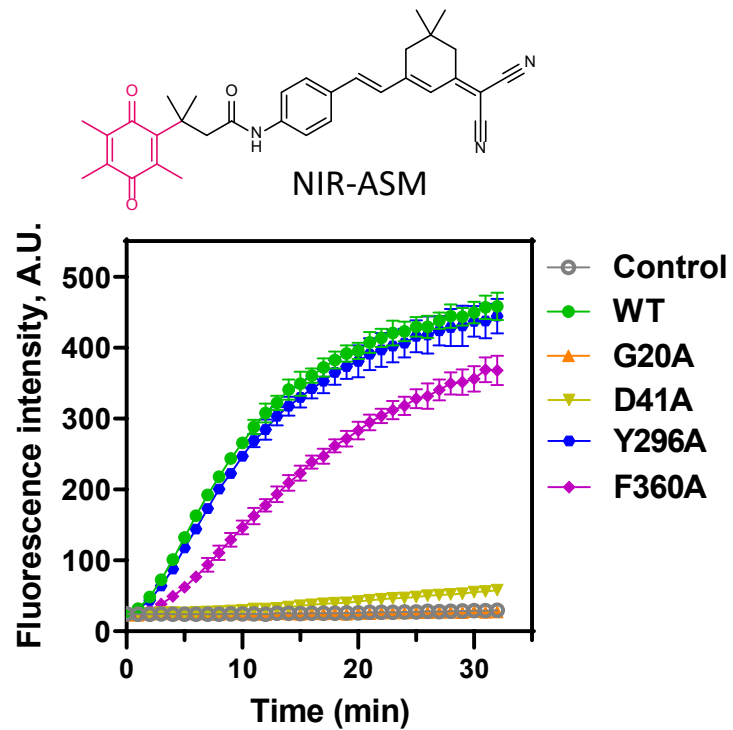
Supplementary Fig. 9 | Structure comparison of FSP1 and yeast Ndi1 and AIF. (a) Superpositions of Ndi1 (pink, PDBcode 4G73) with a bound quinone (raspberry) and apoptosis inducing factor (AIF, PDBcode 4BUR, cornflower blue) onto the AlphaFold model of FSP1 (grey) display differences in the C-termini's surrounding the putative vitamin K (green) binding site. Red arrow denotes deviations between the kinked C-terminal helix of the FSP1 model and the equivalent penultimate helix of Ndi1. The C-terminus of AIF is located away from this position. Black arrow denotes the position of residue F360 located near the vitamin K quinone moiety in the FSP1 model. (b) Global superposition of Nid1 structure with Alphafold model of FSP1. (c) Global superposition of 4BUR with Alphafold model of FSP1.



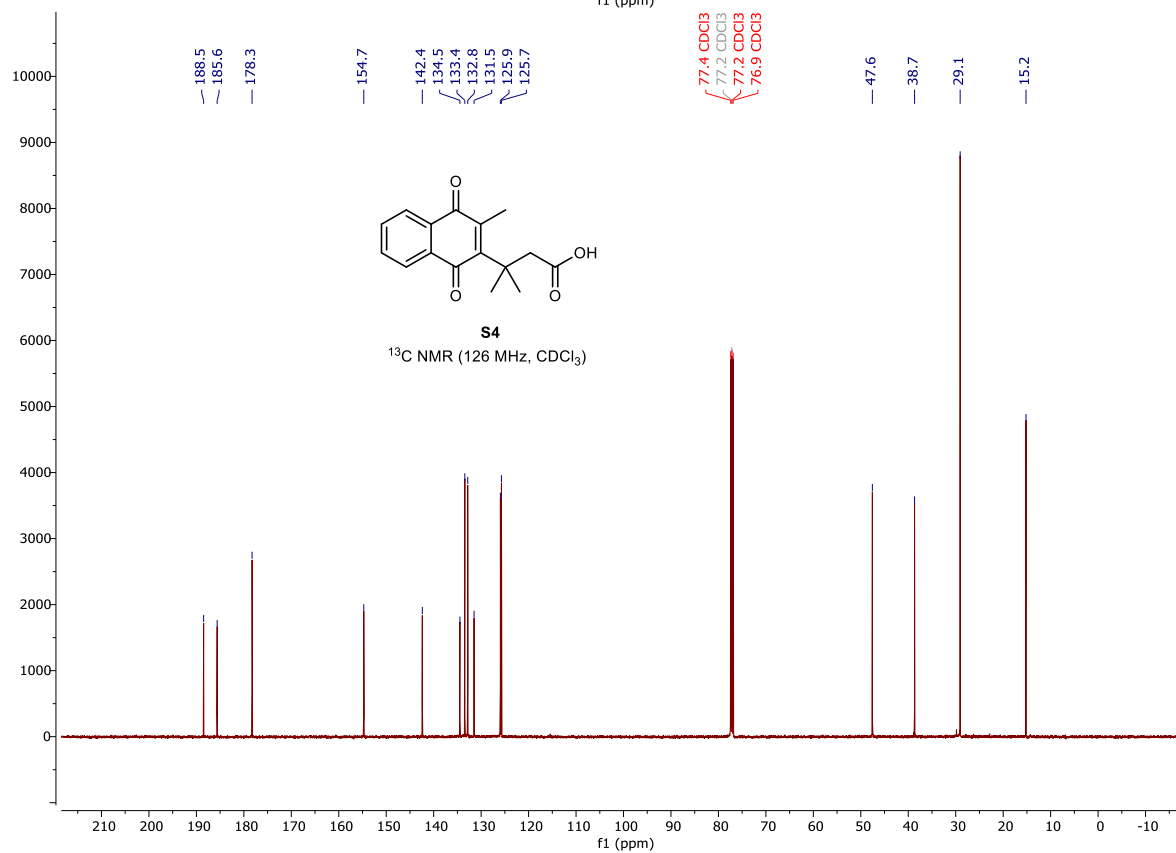
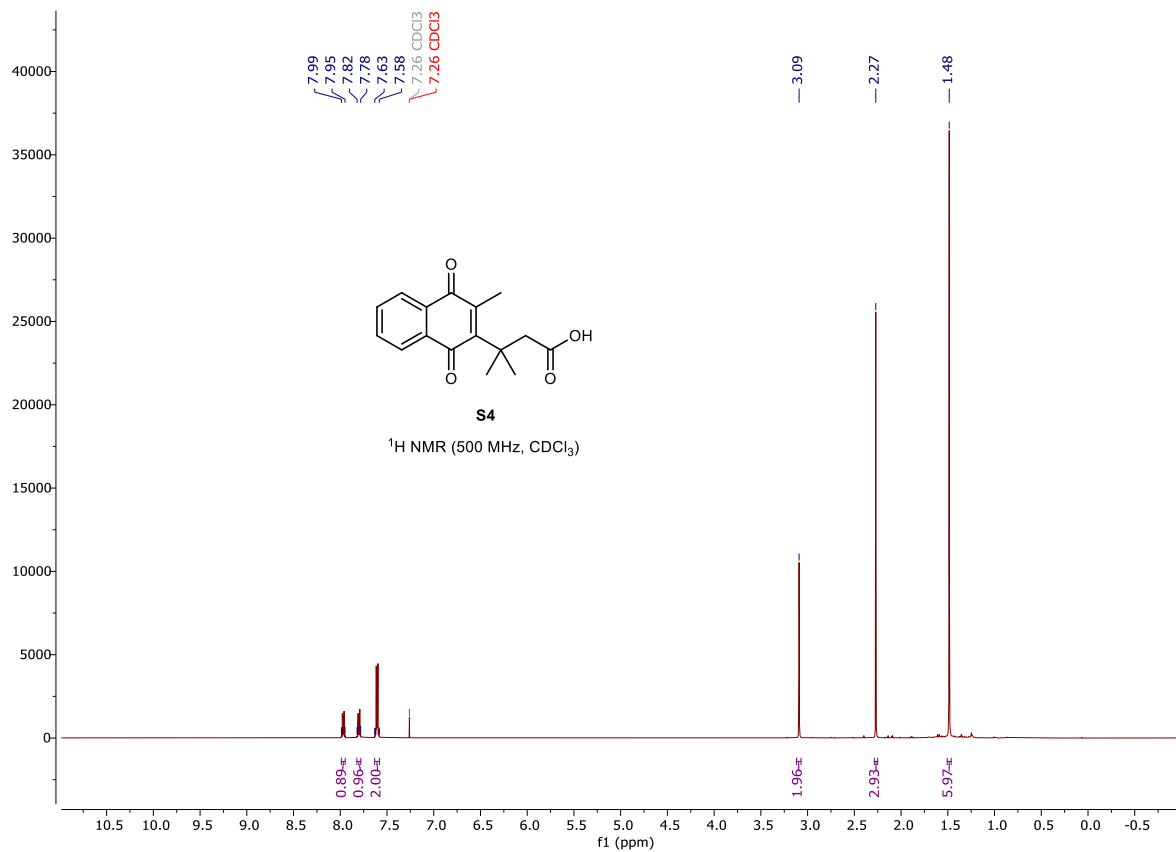
Supplementary Fig. 10 | Synthetic route for VK-ASM (S11).



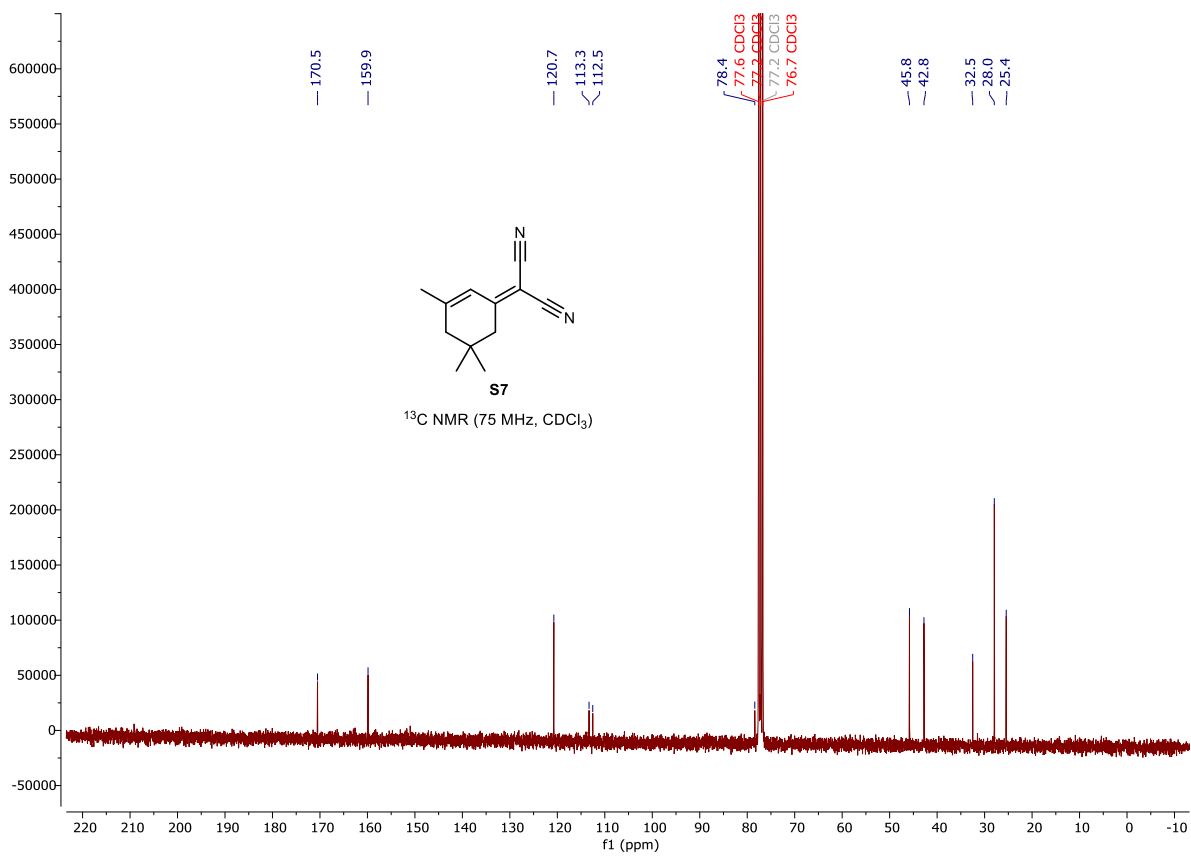
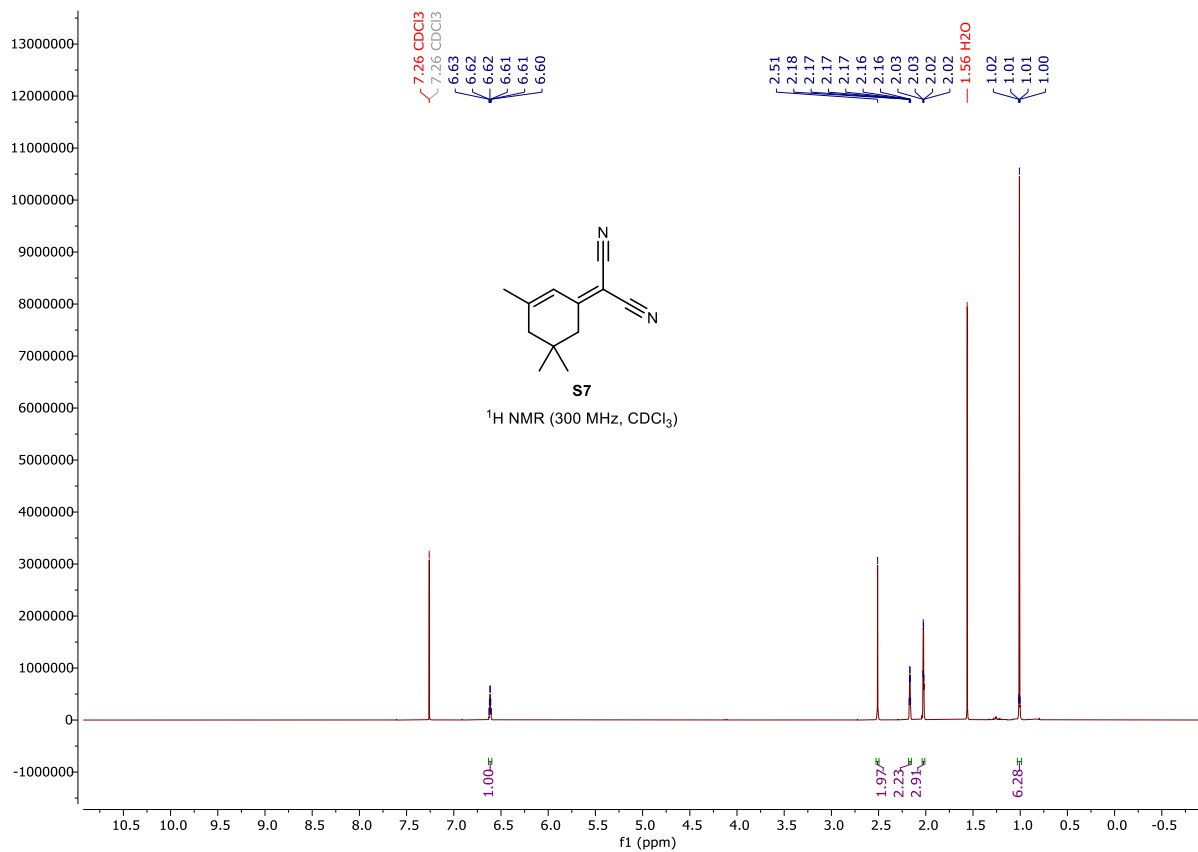
Supplementary Fig. 11 | Activity-based fluorescence probe of vitamin K and ubiquinone for FSP1. (a) Proposed activation mechanism of the activity-based fluorescent probe of ubiquinone (NIR-ASM) towards NQO1. The probe is inactive until the ubiquinone moiety is reduced to hydroquinone, and the rearrangement of the reduced intermediated releases the strong fluorescent tag ASM. (b) Fluorescence emission spectra of the fluorescence tag ASM (blue) and the activity-based probe of vitamin K before activation (orange) excited at 460 nm. Solution measurements were performed in 10×10 mm² quartz cuvettes. Photoluminescence spectra (PL) were measured using Edinburgh Instruments FS5 fluorescence spectrometer in steady-state mode with xenon lamp as the excitation source, exciting at 460 nm.



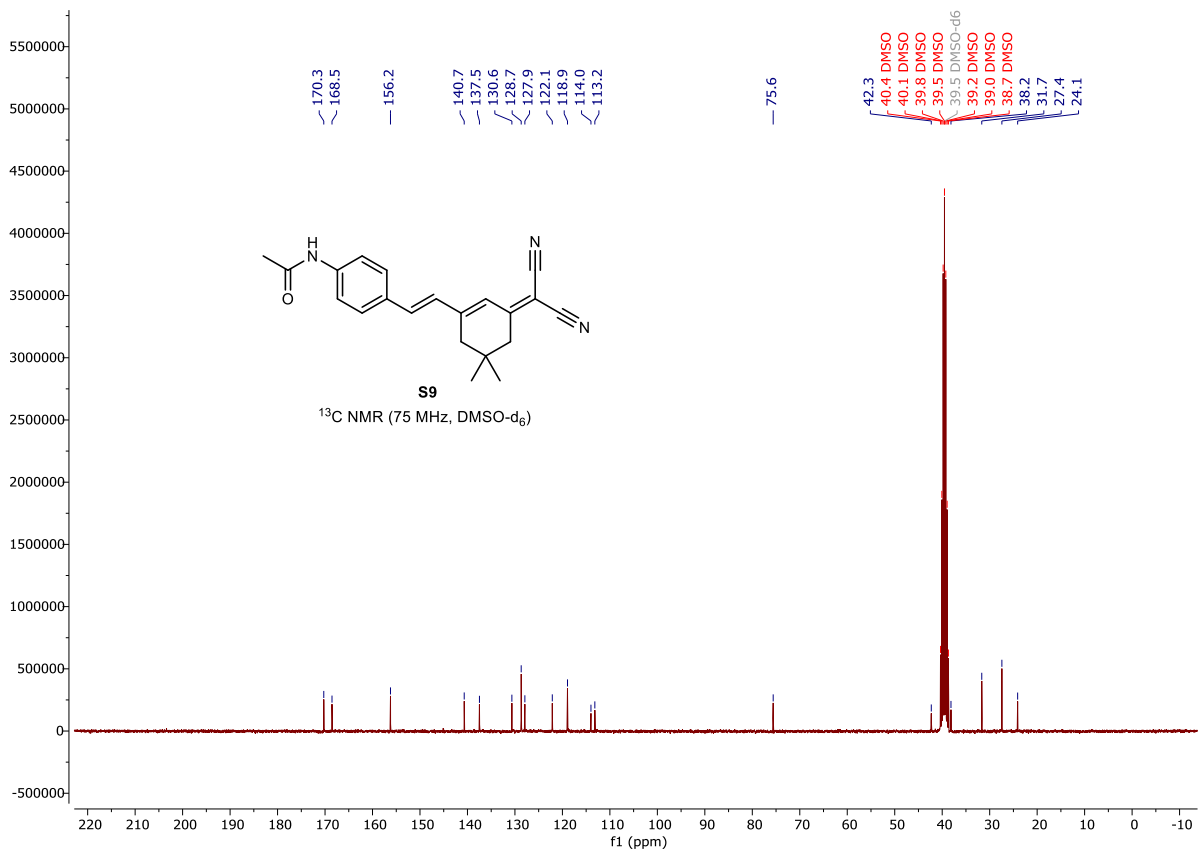
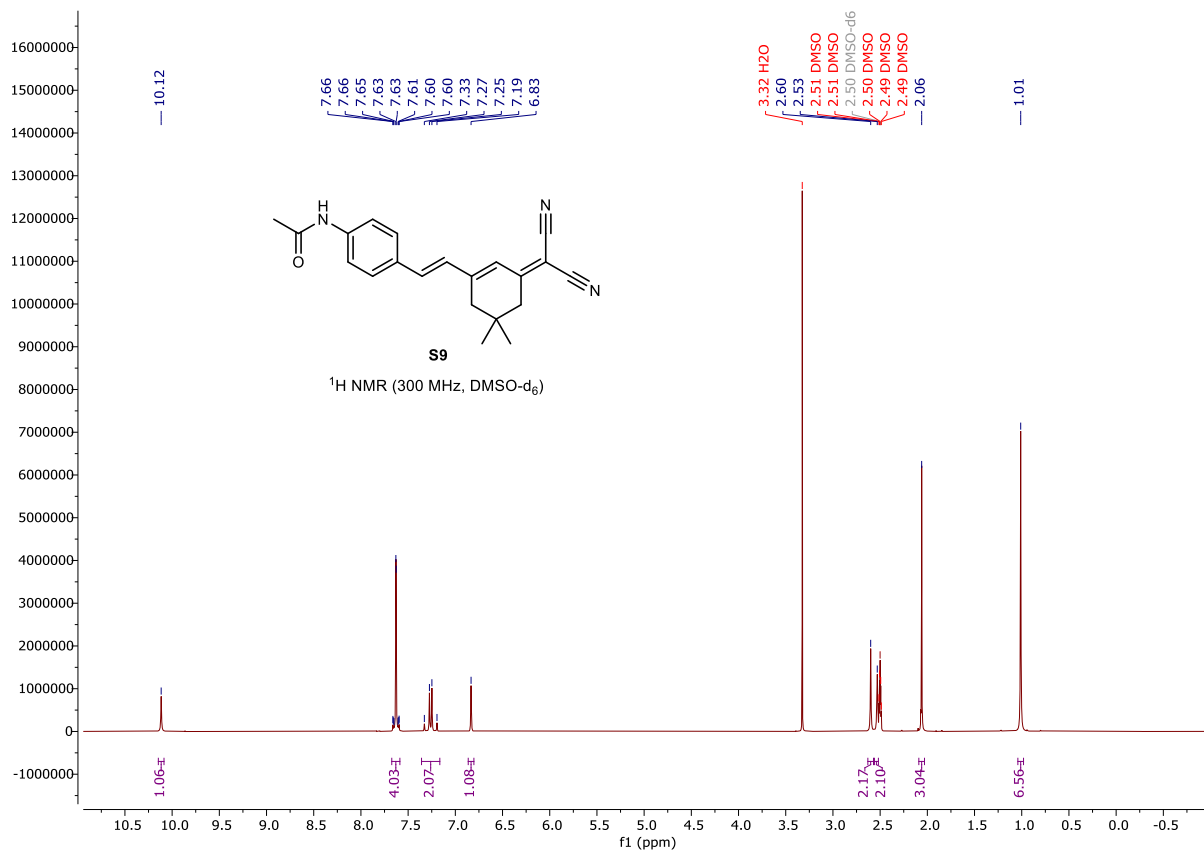
Supplementary Fig. 12 | Comparison of the effect of FSP1 mutations on activity-based fluorescence probes of NIR-ASM and VK-ASM. Wild-type FSP1 or its mutants were transiently expressed in TKO cells and the transfected cells were harvested 48 hours after transfection. Cell lysate was used for activity assays using the fluorescence probe NIR-ASM (**a**) and VK-ASM (**b**) for ubiquinone and vitamin K reduction, respectively, as described in the method section. Control: TKO cells without transfection. Data are presented as mean \pm SD of three independent experiments (n=3).



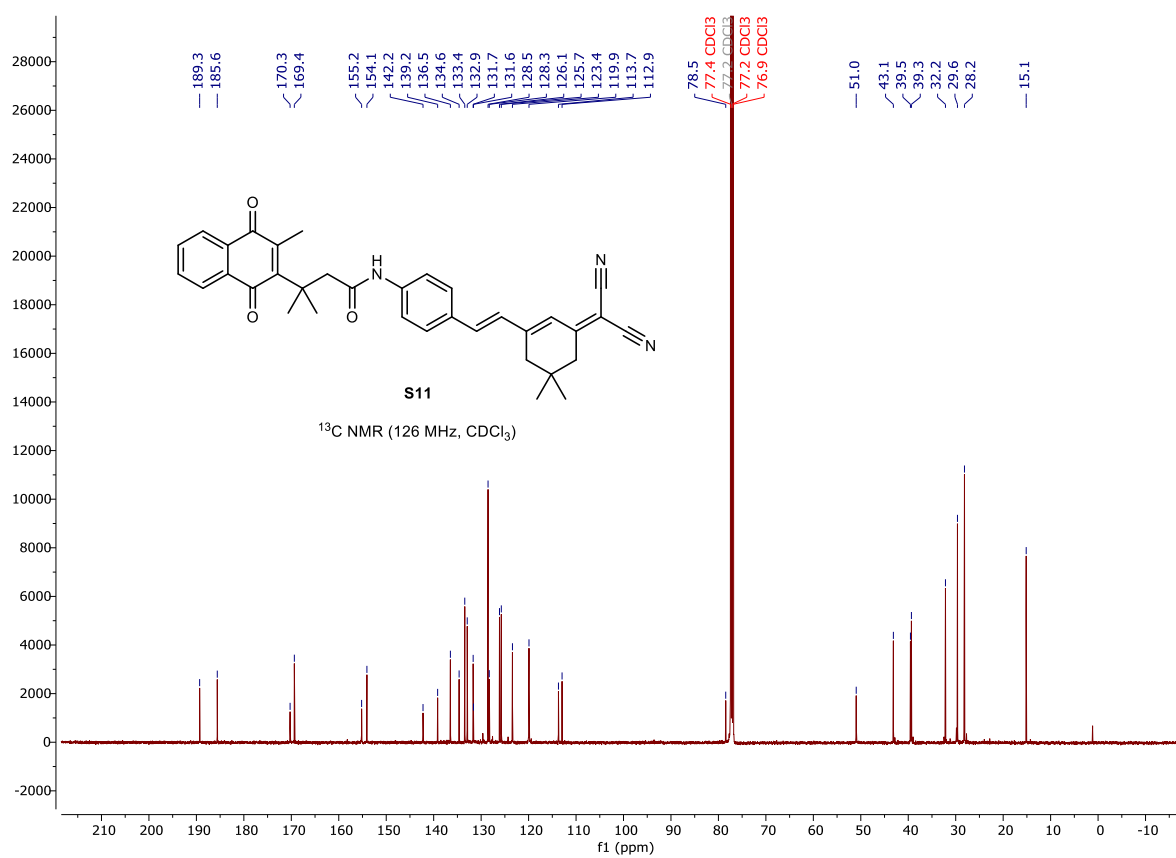
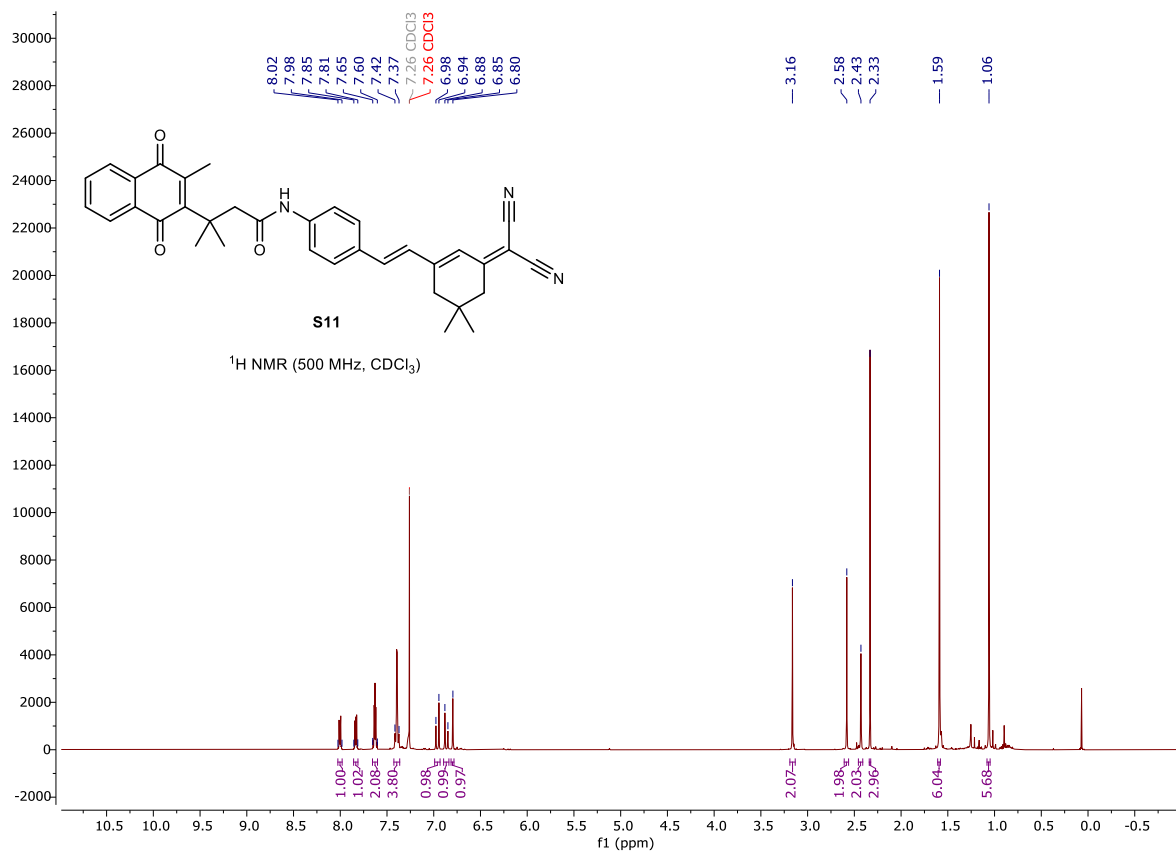
Supplementary Fig. 13 ^1H and ^{13}C NMR spectra of synthetic intermediates (S4, S7, S9) and VK-ASM (S11)



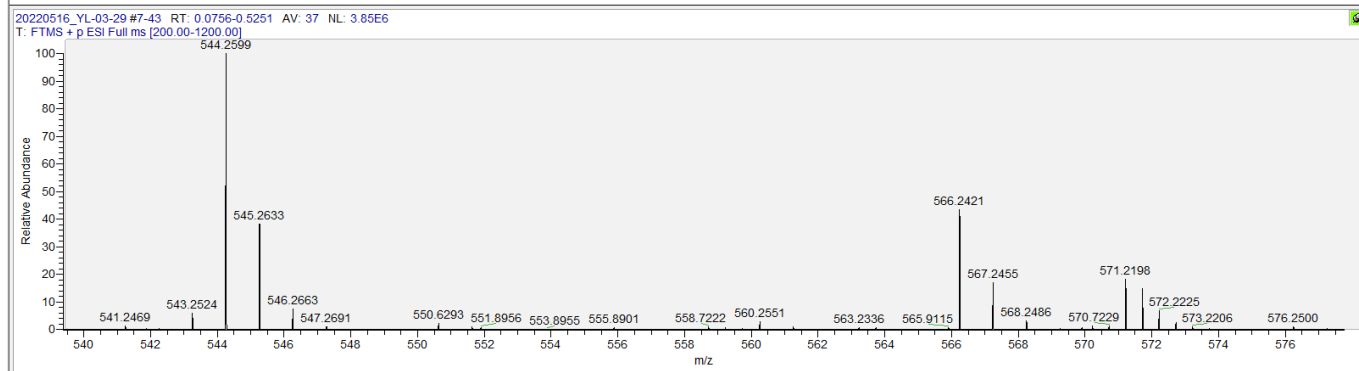
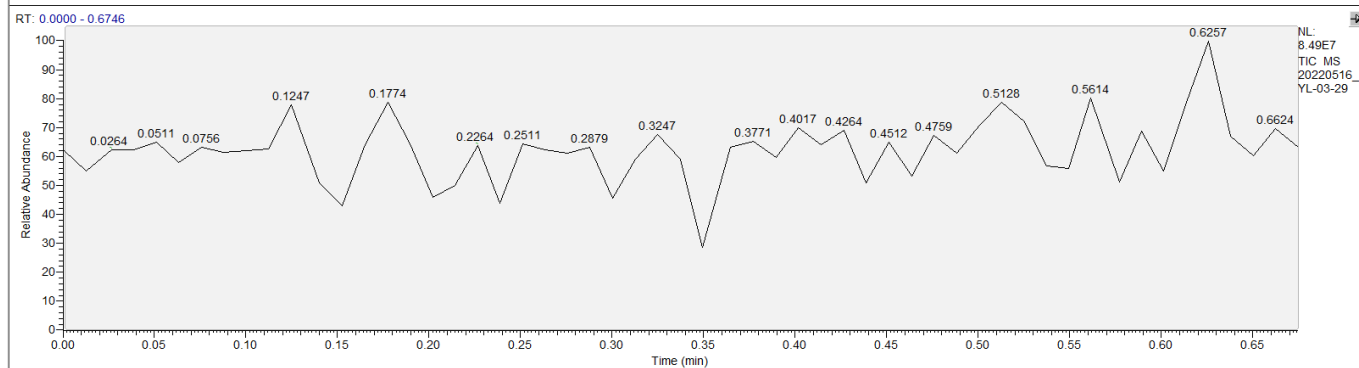
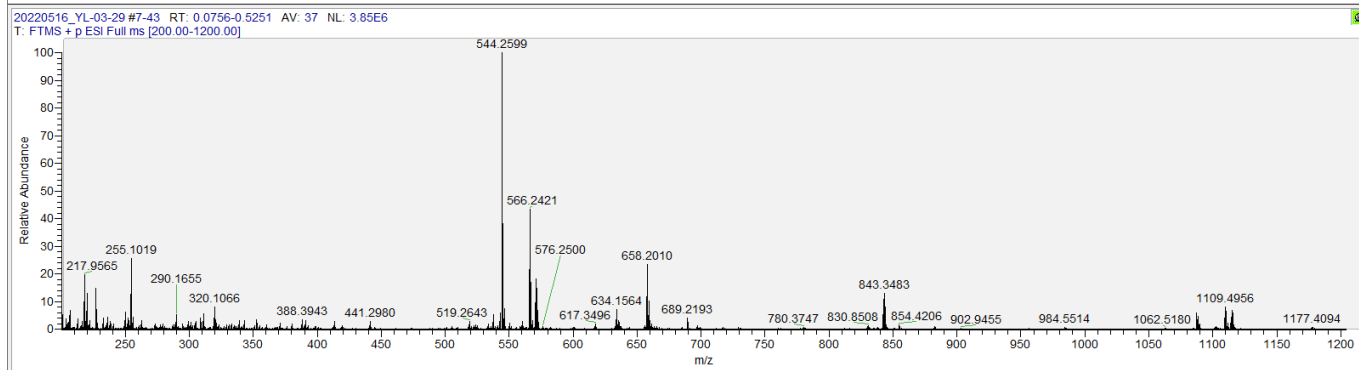
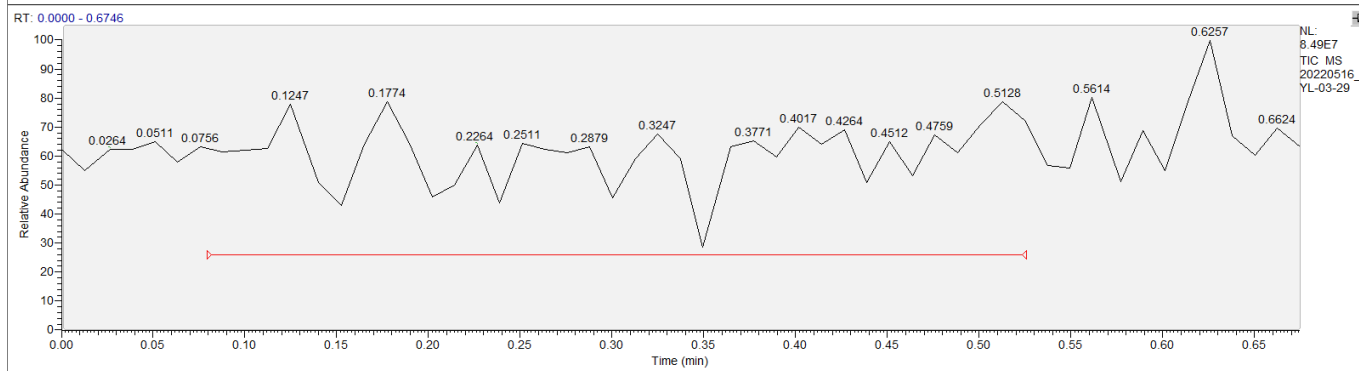
Supplementary Fig. 13 (continued)



Supplementary Fig. 13 (continued)



Supplementary Fig. 13 (continued)



Supplementary Fig. 14 ESI MS Spectra of VK-ASM (S11)